Characterization of three sialidases from *Danio rerio*

Matilde Forcella [a, 1], Marta Manzoni [b, 1], Giuliana Benaglia [b], Marcella Bonanomi [a], Edoardo Giacopuzzi [c, d], Nadia Papini [e], Roberto Bresciani [b], Paola Fusi [a], Giuseppe Borsani [f], Eugenio Monti [b, *]

[a] Dept. of Biotechnology and Biosciences, University of Milano-Bicocca, Milano, Italy
[b] Division of Biotechnology, Dept. of Molecular and Translational Medicine (DMTM), University of Brescia, Brescia, Italy
[c] National Institute for Health Research Oxford Biomedical Research Centre, Oxford, United Kingdom
[d] Wellcome Centre for Human Genetics, University of Oxford, Oxford, United Kingdom
[e] Dept. of Medical Biotechnology and Translational Medicine, University of Milano, Italy
[f] Division of Biology and Genetics, Dept. of Molecular and Translational Medicine (DMTM), University of Brescia, Brescia, Italy

ARTICLE INFO

ABSTRACT

Zebrafish encodes several sialidases belonging to the NEU3 group, the plasma membrane-associated member of the family with high specificity toward ganglioside substrates. Neu3.1, Neu3.2 and Neu 3.3 have been expressed in *E. coli* and purified using the pGEX-2T expression system. Although all the enzymes are expressed by bacterial cells, Neu3.1 formed insoluble aggregates that hampered its purification. Neu3.2 and Neu3.3 formed oligomers as demonstrated by gel filtration chromatography experiments. Actually, the first formed a trimer whereas the second a pentamer. Intriguingly, despite relevant degree of sequence identity and similarity, the two enzymes showed peculiar substrate specificities toward gangliosides other than GM3, two glycoproteins and two forms of sialyllactose. Using molecular modelling and the crystal structure of the human cytosolic sialidase NEU2 as a template, the 3D models of the sialidases from zebrafish have been generated. As expected, the 3D models showed the typical six blade beta-propeller typical of sialidases, with an overall highly conserved active site architecture. The differences among the three zebrafish enzymes and human NEU2 are mainly located in the loops connecting the antiparallel beta strands of the propeller core. These portions of the proteins are probably responsible for the differences observed in substrate specificities, as well as in the different subcellular localization and aggregation features observed in solution. Finally, the *in silico* analysis of RNA-Seq data evidenced a peculiar expression profile of the three genes during embryogenesis, suggesting different roles of these sialidases during development.

1. Introduction

Sialidases (EC 3.2.1.18) are glycohydrolases that removes terminal sialic acid residues from a variety of natural substrates such as oligosaccharides, gangliosides and glycoproteins [1]. These enzymes are widely distributed in nature and a phylogenetic analysis in *Metazoa* revealed new insights on the evolution of this protein family [2]. Starting from the ancestral lysosomal sialidase NEU1, through an intermediate new form called NEU5, the modern membrane associated NEU3/NEU4 followed by the cytosolic NEU2 have evolved. Concerning fish, sialidases have been first characterized at the molecular level in zebrafish (*Danio rerio*) using a transcriptome- and genome-wide search approach and the human NEU polypeptides as queries [3]. Briefly, *neu1* and *neu4* are the orthologues of *NEU1* and *NEU4*, respectively, and other five genes are related to *NEU3*. These are clustered on chromosome 21 and have been named *neu3.1, neu3.2, neu3.3, neu3.4* and *neu3.5*. Temporal expression by RT-PCR revealed the presence of transcripts of all *neu* genes apart from *neu3.4*, with peculiar temporal expression during embryogenesis. Transient expression of some of zebrafish sialidases in COS7 cells revealed different cellular distribution and enzyme activity toward endogenous ganglioside substrates. These results boosted the research in this field of glycobiology with the cloning and characterization of two *neu3* paralogs, as well as *neu4*

and *neu1* from medaka (*Oryzias latipes*) [4—9] and, finally, *neu1, neu3* and *neu4* from Nile tilapia, (*Oreochromis niloticus*) [10—12].

Intriguingly, each enzyme has peculiar features, probably due to the evolutionary path and the role(s) played in different species. On this basis, a detailed biochemical characterization of recombinant Neu3.1, Neu3.2 and Neu3.3 from zebrafish has been carried out. Briefly, the three enzymes expressed in *Escherichia coli* have been successfully purified in the case of Neu3.2 and Neu3.3, and further studied using various experimental approaches, from aggregation state in solution to DANA sensitivity and substrate specificities. In addition, the 3D models of the enzymes have been obtained using homology modelling and the crystal structure of the human cytosolic sialidase NEU2 as a template [13]. Overall, the results obtained provide new insights on sialidases in zebrafish and contribute to a better understanding of the biology of these enzymes in vertebrates.

2. Materials and methods

In general, standard molecular biology techniques were carried out as described by Green and Sambrook [14]. Chemicals, molecular biology reagents, standard molecular weight proteins and culture media were from Sigma (Sigma-Aldrich, Milan, Italy) unless indicated otherwise.

2.1. Expression constructs

cDNAs with the coding region of *neu3.1*, *neu3.2* and *neu3.3* from zebrafish were subcloned into plasmid pGEX-2T (Invitrogen UK Ltd., Paisley, England) according to Ref. [15]. The sequence of the oligonucleotides used to amplify the neu open reading frames that have been cloned in the expression vector are the following: Dr neu3.1-5′ *Bam*HI: 5′-CGGGATCCACCATGTTTTTTACTTACGTTTATG-3′, Dr neu3.1-3′ *Sma*I: 5′-CCCCCGGGGGAGAGCACAA-TAAATCATTAAGT-3'; Dr neu3.2-5′*Sma*I: 5′-CCCCGGGGATG-GAAAAACAACTTGGAAGCA-3′, Dr neu3.2-3′ *Sma*I: 5′-CCCCCGGGGGAATAACCTCTTTGTGTTCAAAC-3′; Dr neu3.3-5′ *Bam*HI: 5′- CGGGATCCACCATGGGCAACAAGACACCGTCAA-3′, Dr neu3.3-3′ *Sma*I: 5′-CCCCCGGGGGCAGCTTTTTCTCAGGGAGTTTG-3'. All the resulting recombinant plasmids were hosted and amplified in *E. coli* strain DH5α. Finally, the constructs were completely sequenced using both vector- and gene-specific primers.

2.2. Recombinant zebrafish sialidase expression and purification

All pGEX-2T constructs were used to transform *E. coli* strain BL21 (DE3). Recombinant Neu3.1, Neu3.2 and Neu3.3 were expressed as GST-fusion proteins. Cells were grown at 37 °C in LB-ampicillin medium and induced at OD_{600nm} equal to 0.8 with 50 μM isopropyl β-D-1-tiogalattopiranoside (IPTG). Different temperatures (15 °C, 25 °C, 37 °C) and induction times (2 h, 4 h, overnight) were evaluated. Cells were harvested by centrifugation for 10 min at 6,000 g and suspended with 50 μL of ice-PBS (10 mM potassium phosphate, pH 7.2, 150 mM NaCl) per mL of initial culture. To obtain crude extract, cells were lysed by sonication in ice (30 s for three times); then Triton X-100 was added at a final concentration of 1% and samples were incubated for 30 min at room temperature. After centrifugation for 30 min at 40,000 g, clarified extracts were obtained. For the purification, extracts obtained after overnight grown at 15 °C were incubated in batch with Glutathione-Sepharose 4B resin (1 mL/g of cells, wet weight) for 30 min at room temperature; the samples were subsequently loaded onto columns for the other steps of the purification procedure. After washing with 20 bed volumes of PBS, for each mL of Glutathione-Sepharose bed volume were mixed 50 μL of thrombin solution (1U/μL) and 950 μL of PBS.

The suspension obtained was incubated in batch overnight at room temperature. Following incubation, the samples were transferred again into columns and the purified proteins were eluted with PBS.

Protein content was evaluated through Bradford assay, using Coomassie Brilliant Blue G-250 and bovine serum albumin as a standard protein.

2.3. Gel filtration chromatography

The aggregation state of sialidases from zebrafish was determined by gel filtration on the Superdex 200 HR 10/300 (GE Healthcare Europe GmbH) column in 50 mM sodium phosphate buffer at pH 7, 150 mM NaCl and the FPLC system. The following proteins were used as standards: apoferritin (443 kDa), β-amylase (200 kDa), alcohol dehydrogenase (150 kDa), bovine serum albumin (67 kDa) and ovalbumin (43 kDa).

2.4. SDS polyacrylamide gel electrophoresis

Sodium dodecyl sulfate polyacrylamide gel electrophoresis (SDS-PAGE) was carried out by standard procedures [16]. For SDS-PAGE, samples were diluted in sample buffer (50 mM Tris-HCl at pH 6.8, 0.4% SDS, 4% glycerol, 1% β-mercaptoethanol and Bromophenol Blue) and heated for 5 min at 95 °C. The samples were loaded onto 4% acrylamide stacking gel (pH 6.8) at 15 mA for 15 min and then electrophoresed onto 12% acrylamide (pH 8.8) at 120 V for 1 h. After electrophoresis, proteins were stained with EZBlueTM Gel Staining Reagent (Sigma-Aldrich, Milan, Italy).

2.5. Western blotting

Protein samples separated by SDS-PAGE were transferred onto a PVDF Immobilon™ P membrane (Millipore, Billerica, MA USA). Membranes were blocked with 5% (w/v) dried milk in PBS overnight at 4 °C. After three washes (10 min each) with PBS containing 0.3% (v/v) Tween 20 (PBS-T) at room temperature, the membranes were incubated with anti-GST rabbit polyclonal antibody (1:4,000) (Sigma-Aldrich, Milan, Italy) diluted in PBS containing 1% (w/v) dried milk and 0.05% (v/v) Tween 20 for 1 h at room temperature. After three washes in PBS-T, membranes were treated for 1 h at room temperature with an anti-rabbit horseradish peroxidase-conjugated IgG (1: 15,000) (Sigma-Aldrich, Milan, Italy) diluted in 5% (w/v) dried milk in PBS. After three washes in PBS-T, detection of antibody binding was carried out with ECL (Amersham GE Healthcare, Uppsala, Sweden), according to the manufacturer's instructions.

2.6. Sialidase enzymatic assays

The enzymatic activities of recombinant Neu3.1, Neu3.2 and Neu3.3 from zebrafish were evaluated with the artificial substrate 4MU-NANA and on the natural substrates α(2—3)sialyllactose, 3-sialyllactose, fetuin, mucin, GM1, GM3, GD3 and GD1a gangliosides.

The enzymatic activity on 4MU-NANA was determined with a fluorimetric method according to Tringali et al. [17]. Briefly, reactions were set up at least in triplicate using different amounts of proteins in 25 mM Na citrate/phosphate buffer, pH 5.6, 0.1 mM 4MU-NANA, 6 mg/mL BSA, in a final volume of 100 μL. After incubation for 30 min at 37 °C, reactions were stopped by adding 1.5 mL of 0.2 M glycine/NaOH, pH 10.8. The enzyme activity was evaluated by spectrofluorimetric measurement of the 4-MU released, with excitation at 365 nm and emission at 445 nm. Kinetic constants were obtained by measuring enzymatic activity at different 4MU-NANA concentrations, from 0.04 to 0.2 mM. K_m and V_{max} values were determined by the method of Lineweaver-Burk. To measure

the inhibitory constant K_i of 2,3-dehydro-2-deoxy-*N*-acetylneuraminic acid (DANA), the same experiments were carried out in the presence of two different competitive inhibitor concentration, namely 0.2 and 0.4 mM. To obtain the K_i value, the kinetic data were fitted to the equation for competitive inhibition.

The enzymatic activity on α(2−3) sialyllactose, 3-sialyllactose, fetuin, mucin and GM1, GM3 and GD3 gangliosides was determined as described below [17]. Reactions were setup at least in triplicate using 5 μg protein, in 25 mM Na citrate/phosphate buffer, pH 5.6, containing 50 μg α(2−3)sialyllactose or 3-sialyllactose, in a final volume of 100 μL (0.75 mM final concentration). An amount of fetuin or mucin corresponding to 50 μg of sialic acid was used under the same reaction conditions described above. An amount of GM1, GM3 and GD3 ganglioside corresponding to 60 nmol was dissolved in a chloroform/methanol 2:1 (v/v) solution. Before setting up the reaction mixture, the solvent was completely removed by nitrogen fluxing; the residues were then dissolved in a specific amount of redistilled water (30 μL/reaction), the Triton X-100 was added at final concentration of 0.04% and the mixture was incubated for several hours at room temperature to facilitate the micellar aggregation. The reactions were set up in a final volume of 100 μL (0.6 mM final concentration), as described above. After incubation for 1 h at 37 °C, released sialic acid was separated on an ion-exchange chromatography on Dowex 238 resin (100−200 mesh) (Sigma-Aldrich, Milan, Italy) and assayed with a chemical method according to Warren [18]. The amount of released sialic acid was determined by a spectrometric measurement of the sample absorbance of at 532 and 550 nm.

For the enzymatic activity on GD1a, the incubation mixtures (100 μL), containing 0.6 mM of micellar ^{3}H-labeled ganglioside GD1a carrying 0.15 Ci of radioactivity and in the presence of 0.04% Triton X-100, were incubated at 37 °C with recombinant sialidases for 1 h. The incubations were terminated by cooling the tubes in an ice bath, adding 400 μL of tetrahydrofuran and careful vortexing. The mixtures were then centrifuged at 10,000 g for 5 min, and 5 μL of the resulting supernatants were subjected to HPTLC on silica gel plates with chloroform, methanol, 0.2% aqueous CaCl$_2$ (50:42:11, v/v/v) as a solvent system to separate the reaction products from the substrates. The separated glycolipids were quantified by radiochromatoscanning (Beta Imager 2000, equipped with the software interface Beta Vision, Dell Optiplex Systems, Biospace Mesures, Paris, France), and the enzyme activity was calculated as already reported [19].

2.7. Molecular modelling

The maltose-induced structure of human cytosolic sialidase NEU2 [13] was retrieved from RCSB Protein Data Bank (https://www.rcsb.org/) [20] under accession 1SO7 and used as template for all protein models. Structural models were constructed using *HHpred* and *Modeller* [21] with NEU2 as template. The PDB structures obtained were visualized, aligned and manipulated using PyMol (The PyMOL Molecular Graphics System, Version 2.1, Schrodinger, LLC).

2.8. Prediction of membrane spanning regions or myristoylation

The amino acid sequences of Neu3.1, Neu3.2 and Neu3.3 have been analyzed with several bioinformatic tools in order to find possible explanation(s) to their different behavior as recombinant proteins expressed in *E. coli*. Prediction of possible membrane spanning regions has been assessed using TMPred (https://www.expasy.org/resources/tmpred), TMHMM Server v. 2.0 (http://www.cbs.dtu.dk/services/TMHMM/), PSIPRED MEMSAT-SVM (http://bioinf.cs.ucl.ac.uk/psipred/) and SOSUI (https://harrier.nagahama-i-bio.ac.jp/sosui/sosui_submit.html). Prediction of possible *N*-terminal myristoylation has been assessed using Myristoylator (https://web.expasy.org/myristoylator/).

2.9. In silico zebrafish sialidase gene expressiom

Zebrafish sialidase gene expression data have been derived from RNA-seq experiments carried out in the Busch-Nentwich laboratory across 18 time points from 1 cell to 5 days post-fertilization sampling individual and pools of embryos [22]. Normalized transcript counts per gene, expressed as Transcripts Per Million (TPM), have been extracted from the EMBL-EBI Expression Atlas at the following address http://www.ebi.ac.uk/gxa/experiments/E-ERAD-475.

3. Results

3.1. Expression of Neu3.1, Neu3.2 and Neu3.3 from zebrafish in Escherichia coli

To obtain a large amount of Neu3.1, Neu3.2 and Neu3.3 polypeptides from zebrafish we subcloned the ORF of the three genes in the pGEX-2T bacterial expression vector as described in *Materials and methods*. After transformation of *E. coli* BL21 cells, the polypeptides were expressed as glutathione S-transferase fusion proteins upon induction with 50 μM IPTG. As expected, new protein bands with an apparent molecular mass of about 72.4, 68.7 and 71.5 kDa, corresponding to Neu3.1, Neu3.2 and Neu3.3, respectively, appeared after SDS-PAGE separation of the transformed bacterial extracts, indicating expression of the fusion proteins (Supplementary figs 1-3). Moreover, specific immunoreactive bands were detected by Western-blotting using anti-GST antibody. A detailed analysis of the expression pattern detectable under different temperatures and induction periods revealed that 15 °C and overnight induction were the best conditions as a compromise between the overall yield and the almost complete absence of low molecular weight degradation products.

3.2. Purification of recombinant neu3.1, neu3.2 and neu3.3

Briefly, batch purification of glutathione S-transferase-Neu3.1, Neu3.2 and Neu3.3 fusion proteins, followed by thrombin cleavage as described in Materials and Methods section, was carried out. Although GST-Neu3.1 was expressed and detectable in *E. coli* extracts, the fusion protein was not able to recognize glutathione immobilized on GSH-Sepharose 4B; thus, purification of the enzyme failed. The presence of a great part of the protein in the bacterial pellet strongly support the notion that GST-Neu3.1 was embedded within inclusion bodies. In addition, the minor GST-Neu3.1 aliquot detectable in crude soluble extracts probably formed complexes that hampered the recognition of GSH by the GST portion of the protein chimera during the affinity chromatography purification step (data not shown). The overall picture remained unaltered by using urea, guanidine hydrochloride or other detergents with null or only minor amount of Neu3.1 chimera detectable in soluble fractions. Also in these experimental conditions, recombinant GST-Neu3.1 was unable to bind on GSH-Sepharose 4B and no sialidase activity was detectable using 4MU-NANA as substrate (not shown). Conversely, affinity purification of recombinant Neu3.2 and Neu3.3 succeeded. Briefly, Neu3.2 showed the enrichment of a major band with the expected molecular mass of about 42.8 kDa after GST removal with thrombin. Another protein band with a molecular mass of about 33.7 kDa was also detected, probably corresponding to a degradation product. In addition, two other minor protein bands with a molecular weight

higher than 95 kDa were also detected (Fig. 1A). A purification yield of 30% was estimated, as well as a purification factor corresponding to 70 folds, compared to the sialidase specific activity detectable in the starting crude bacterial extract (Table 1).

Concerning Neu3.3, the purification procedure showed the enrichment of a band with the expected molecular weight of about 45.8 kDa, with other minor protein contaminants with dimensions ranging from 28 to 120 kDa (Fig. 1B). The purification yield was about 60%, with a high purification factor that, compared to the sialidase specific activity detectable in the starting crude bacterial extract, corresponded to 94 folds (Table 1).

3.3. Aggregation state of recombinant Dr Neu3.2 and Dr Neu3.3 in solution

To study the aggregation state of these two purified sialidases, the enzymes were subjected to gel filtration chromatography using the FPLC system and the appropriate set of standard proteins (Fig. 2). In these conditions, the sialidase Dr Neu3.2 was present as an aggregate with a calculated molecular mass of 134 kDa, indicating that the enzyme formed a trimer. Concerning Dr Neu3.3, its calculated molecular mass in gel filtration chromatography corresponded to 217 kDa: thus the enzyme, at least in these experimental conditions, aggregated and showed the molecular mass of a pentamer.
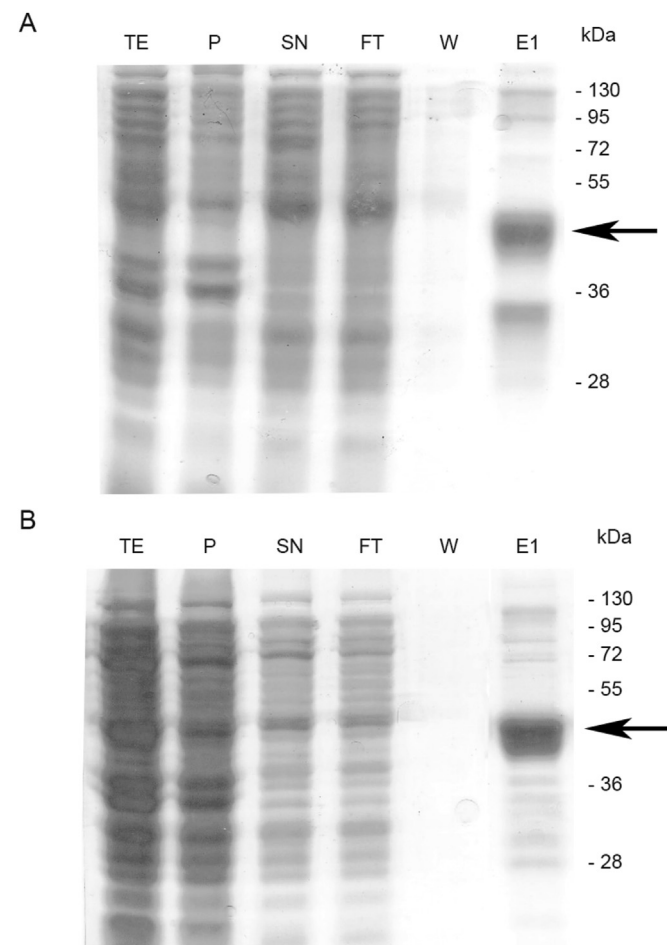

Fig. 1. Purification Neu3.2 (A) and Neu3.3 (B). Protein samples were separated by SDS-PAGE: 20 μg of total extract (TE), pellet (P), 15 μg of supernatant (SN), 12 μg of flow through (FT), 5 μg of wash (W), 3 μg of first elution (E1). The arrow indicates the protein purified.

3.4. Sequence analysis of Neu3.1, Neu3.2 and Neu3.3

On the basis of the different behavior of the paralogs in the *E. coli* expression system, as well as on their aggregation properties in solution and on the previously reported subcellular localization upon transient expression in COS7 cells [3], the amino acid sequences of the three sialidases have been further analyzed using bioinformatic resources. TMPred and TMHMM, did not revealed any possible transmembrane (TM) helices with significant scores. SOSUI predicted Neu3.2 and Neu3.3 as soluble proteins, whereas it predicted the first 23 amino acid of Neu3.1 as a TM helix. PSIPRED predicted TM portions for all the paralogs: Neu3.1 has a TM portion spanning residues 43—56, with an extracellular *N*-terminus and a cytoplasmatic portion from residue 57 to the C-terminus; Neu3.2 and Neu3.2 have TM portions spanning residues 337—352 and 365—380, respectively, with the same topology described for Neu3.1. All these predictions are not compatible with the highly conserved six blade β-propeller 3D structure typical of sialidases [13,23]. Finally, Myristoylator did not identified any Gly residue at the *N*-terminus that could be modified by addition of myristate in the paralogs. These results, together with the sequence analysis reported by Manzoni et al. [3], do not support significant explanation for the general features (e.g. clusterization in inclusion bodies, aggregation capability and subcellular localization) observed in the three paralogs.

3.5. Characterization of recombinant Neu3.2 and Neu3.3 toward various substrates

Purified recombinant Neu3.2 and Neu3.3 was used as enzyme source to characterize their ability to remove sialic acid from different substrates, namely GD1a, GD3, GM3 and GM1 gangliosides, fetuin, mucin and two types of oligosaccharides, namely α(2—3) sialyllactose and 3-sialyllactose, as reported in Fig. 3.

The results obtained clearly demonstrated that the two enzymes showed peculiar substrate specificities. All the gangliosides tested were recognized as substrates, although with surprising differences. First of all, in the case of Neu3.2 GM1 was the best substrate, followed by GD3, GD1a and GM3, whereas in the case of Neu3.3, GD3 was the best substrate, followed by GD1a, GM1 and GM3, being the last the less acknowledged, with an activity superimposable in the two paralogs toward these three gangliosides. In addition, both the enzymes removed sialic from the glycoprotein fetuin whereas sialidase activity toward the glycoprotein mucin was detectable only when using recombinant Neu3.2 as enzyme source. Finally, the trisaccharide sialyllactose showed again that the paralogs have peculiar features. Actually, 3-sialyllactose bearing *N*-acetyl group on C5 of sialic acid was equally recognized by Neu3.2 and Neu3.3, whereas α(2—3) sialyllactose, characterized by the free amino group on C5, was poorly recognized by Neu3.3. Overall, Neu3.2 was highly active toward GM1, followed by GD3 (50% of the previous one), whereas in case of GD1a and GM3 the activity detected was considerably low if compared to GM1, corresponding to 9 and 2%, respectively. Such very low values of enzyme activity were detectable in the case of fetuin and mucin, whereas the two forms of sialyllactose were much better substrates with values corresponding to roughly 14—15% of the one observed with GM1. Concerning Neu3.3, GD3 was the best substrate with an activity corresponding to one half of the one observed in the case of the other paralog, followed by GD1a and GM1 with an activity corresponding to 20% of the one observed with GD3, whereas in case of GM3 the activity was further halved. As already mentioned, Neu3.3 was less active than Neu3.2 on fetuin and, at least in the experimental condition used in this study, was unable to remove sialic acid residues from mucin. Finally, Neu3.2 showed an activity

Table 1
Purification of recombinant Dr Neu 3.2 and Neu3.3

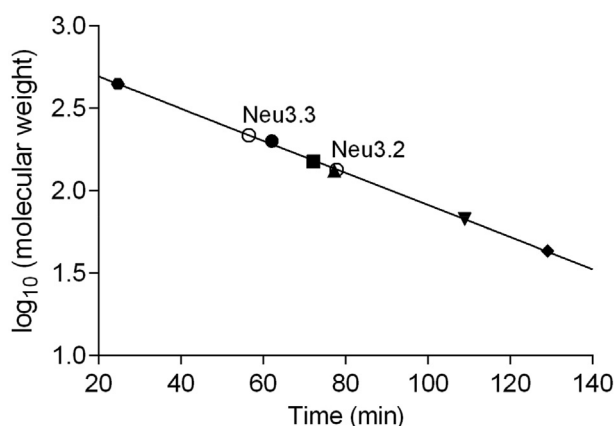| Enzyme		Vol (mL)	Relative activity (nmol/h mL)	Total activity (nmol/h)	Protein concentration (mg/mL)	Specific activity (nmol/h mg)	Yield (%)	Purification Index (Fold)
Neu3.2	Total extract	26	106	2755	4.67	22.70	100	1
	Affinity chromatography	2	411	822	0.26	1581	30	70
Neu3.3	Total extract	17	97.5	1657	3.85	25.32	100	1
	Affinity chromatography	2	550	1100	0.23	2391	66	94

Fig. 2. The aggregation state of recombinant Neu3.2 and Neu3.3. Aliquots of the purified recombinant enzymes (○) were subjected to gel filtration analysis on Superdex 200 HR 10/300. Calibration curve was obtained using the following proteins as molecular weight standards: apoferritin 443 kDa (□), β-amylase 200 kDa (●), alcohol dehydrogenase 150 kDa (■), albumin as monomer 67 kDa (▼) and dimer 134 kDa (▲) and ovalbumin 43 KDa (◆). For details see Material and Methods.
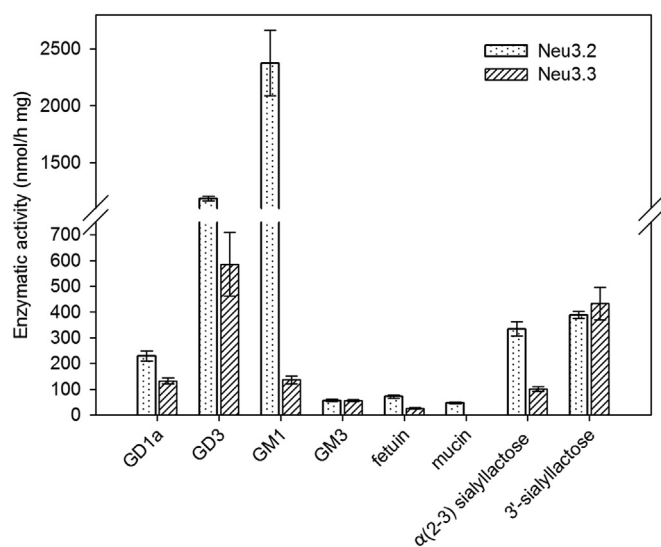

Fig. 3. Sialidase activity of purified recombinant Neu3.2 and Neu3.3 toward the natural substrates GD1a, GD3, GM1 and GM3 ganglioside, fetuin, mucin, α(2,3) sialyllactose and 3-sialyllactose. Values are means ± SD of three independent experiments.

toward 3′-sialyllactose corresponding to 70% of the value observed with GD3, roughly 3.5 higher than the one observed for GD1a and GM1.

These peculiar kinetic features should be explained by differences of the active site architecture and/or recognition of substrates by portions of the enzymes that surround the active site crevice.

3.6. Measurements of the kinetic constants and Ki of DANA on recombinant Neu3.2 and Neu3.3

To better characterize these two recombinant sialidase from zebrafish, typical Vo/[S] experiments were carried out, using 4MU-NANA as substrate, obtaining the Vmax and Km values. In addition, Ki values for the competitive inhibitor DANA have been calculated by using the double reciprocal plot, two DANA concentration and the resulting kinetic data interpolated to competitive inhibitor equation (Fig. 4). Briefly, Vmax values of the two paralogs expressed as nmol of sialic acid released/h μg were roughly similar, being Neu3.2 slightly more active than Neu3.3, whereas in the case of Km, Neu3.2 showed an higher affinity, with a value of roughly one/third compared to the one observed in case on Neu3.3. Finally, the observed Ki values for the two recombinant zebrafish sialidases were found similar and superimposable with the inhibitory constant measured for DANA in case of HsNEU2 [24]. Overall, whereas the Km values measured for the two zebrafish paralogs were of comparable to the one observed in HsNEU2, the Vmax values were very low, corresponding roughly to 6–8% of the corresponding kinetic parameter measured using the recombinant human cytosolic sialidase NEU2 as enzyme source [17].

3.7. Structural features of Neu3.1, Neu3.2 and Neu3.3 deduced by molecular modelling

Based on the different behavior of zebrafish Neus upon their production as GST fusion proteins in *E. coli*, as well as on their substrate specificity and aggregation capacity, we decided to generate the 3D models of the enzymes using Modeller [25] and the maltose induced structure of the human cytosolic sialidase NEU2 (PDB: 1so7) as a template [13]. As expected from the high level of sequence identity [3], as well as from previous evolutionary study carried out on this glycohydrolase enzyme family [2], the 3D models obtained closely resemble the crystal structure of NEU2, with the six-blade β-propeller typical of sialidases [23] (Fig. 5). Differences are mainly located in the connection loops between the antiparallel β-strands of the β-propeller, as well as in the flexible (and divergent or not conserved) *N*-terminal and C-terminal portions.

The active site architecture is highly conserved (Fig. 6), with the Arg triad and the other residues involved in the catalysis and substrate recognition in topologically equivalent positions [2]. In Dr Neu3.1, Neu3.2 and Neu3.3 structural models, the residues corresponding to Asp 46 and Glu 111 in NEU2 are located far away from the active site crevice, as expected from the maltose induced structure of NEU2 (PDB: 1SO7) used as a template (Fig. 7A). Concerning the loops connecting the antiparallel β-strands, Dr Neu3.3 shows a longer stretch of residues between the B and C sheets of the third blade of the propeller compared to Dr Neu3.1, Neu3.2 and Hs NEU2 (Fig. 7B). In addition, Dr Neu3.1 has a more consistent insertion between sheets A and B of the fifth blade of the propeller on the opposite site of the active site (Fig. 7C), whereas in the sheets
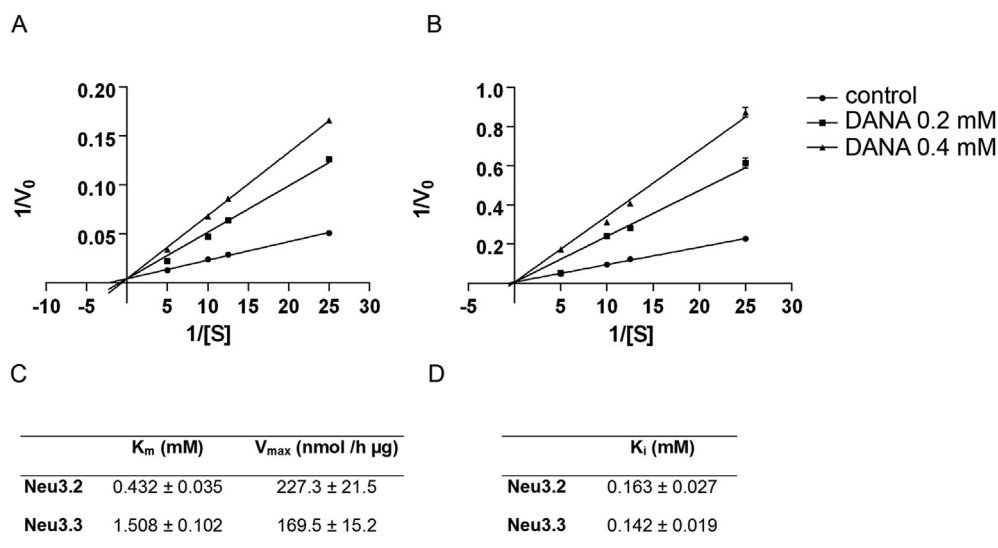
Fig. 4. Inhibition assay of zebrafish Neu3.2 and Neu3.3. Sialidase activity of Neu3.2 (A) and Neu3.3 (B) was measured using 4MU-NANA as substrate (control) and in presence of two concentrations of the competitive inhibitor DANA. The kinetic parameters Km and Vmax for the artificial fluorescent substrate of the two paralogs and the corresponding Ki values are reported in C and D, respectively.
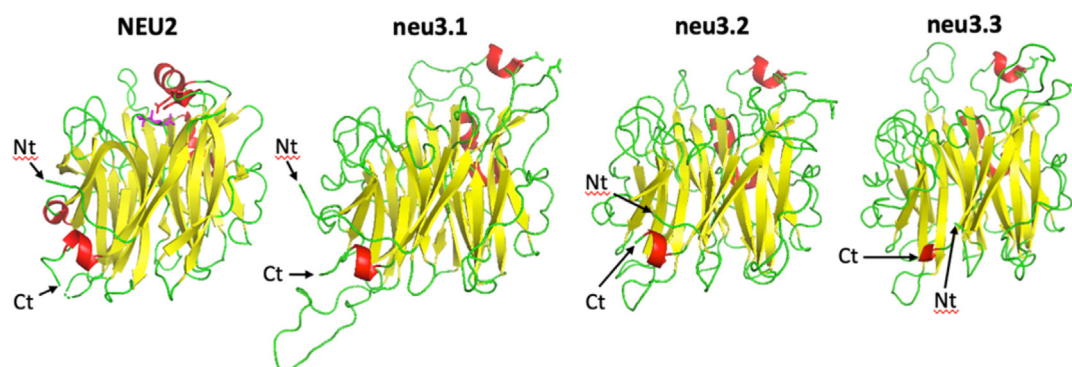

Fig. 5. Ribbon diagram of Hs NEU2 and Dr Neu3.1, 2 and 3 viewed by the side. The active site is located on the top part of the proteins; NEU2 structure (left) shows the competitive inhibitor DANA (violet), as well as the side chain of Asp 46 and Glu 111 (red) located in the mobile loops bearing α1 and α2 helices (PDB code 1VCU). The 3D structural features of the Dr Neus obtained by molecular modelling show a more complex network of unordered segments. The amino and carboxy terminus are indicated by Nt and Ct, respectively. Color code: β-strands yellow; α-helix red; unordered green.

A, B and C of the sixth blade of the propeller differences are not so pronounced and localized mainly on the opposite site of the active site (Fig. 5).

4. Discussion

Sialidases from *Danio rerio* have been the first members of the enzyme family characterized in bony fishes [3]. From 2013, several sialidases have been cloned in different fishes, from *Oryzias latipes* (medaka) to *Oreochromis niloticus* (Nile tilapia) [4—6,8—12]. The characterization of these new members of the sialidase family prompted us to a more detailed study of some of the Neu3 enzymes of zebrafish, namely Dr Neu3.1, Neu3.2 and Neu3.3. As already reported, multiple alignment of these *D. rerio* sialidases and the human cytosolic sialidase NEU2 clearly shows the presence of highly conserved amino acid stretches along the polypeptides, with differences mainly located in the loops between the antiparallel β-strands of the propeller, as observed in our phylogenetic analysis of the sialidase protein family in Metazoa [2]. Moreover, Asp boxes and the amino acid that in NEU2 are involved in DANA coordination and form the active site are detectable in topologically equivalent

positions in the three sialidase from zebrafish [3]. Surprisingly, despite the high degree of similarity with the other sialidases involved in this study, recombinant Dr Neu3.1 expressed in *E. coli* remained in the bacterial inclusion bodies and its purification failed; the reason of this irreversible aggregation is not clear, at least based on the sequence analysis carried out using various bioinformatic tools. On the contrary, Dr Neu3.2 and 3.3 were successfully purified using the standard protocols recommended for pGEX expression vector. Neu3.1 predicted 3D structure (Fig. 5) showed a long loop between sheets A and B of the fifth blade of the propeller, localized on the opposite site of the active site (Fig. 7C). Accumulation of recombinant proteins in *E. coli* inclusion bodies has been studied in the case of human growth hormone and bacterial asparaginase, demonstrating the important role played by hydrophobic interactions between partially folded amphiphilic and hydrophobic alpha-helices in the aggregation [26]. It is tempting to speculate that these peculiar structural features, and/or other more subtle differences on the enzyme surface, are responsible for Dr Neu3.1 clusterization in inclusion bodies. In addition, purified Dr Neu3.2 and Neu3.3 formed aggregates when in solution, as demonstrated by the gel filtration chromatography experiments
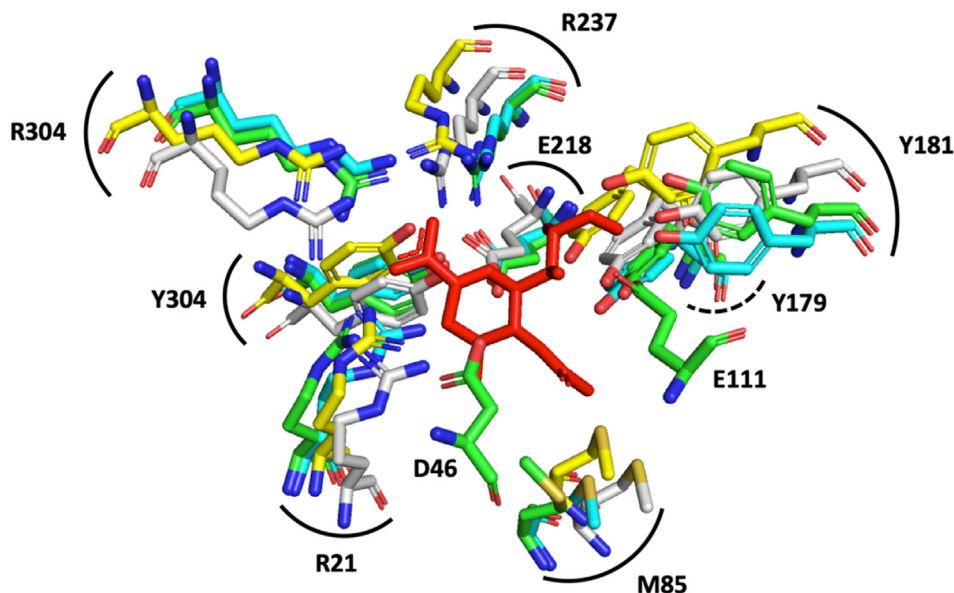
Fig. 6. Overlay of the amino acid residues in the active site crevice of Hs NEU2/DANA complex (PDB ID 1VCU) with the predicted 3D structures of Dr Neu3.1, 2 and 3. View from the top: the carbon backbone of the active site residues of Hs NEU2, Dr Neu3.1, Dr Neu3.2 and Dr Neu3.3 are colored in green, light blue, grey and yellow, respectively, whereas the competitive inhibitor DANA is colored in red. The amino acid numbers are referred to Hs NEU2 [13].
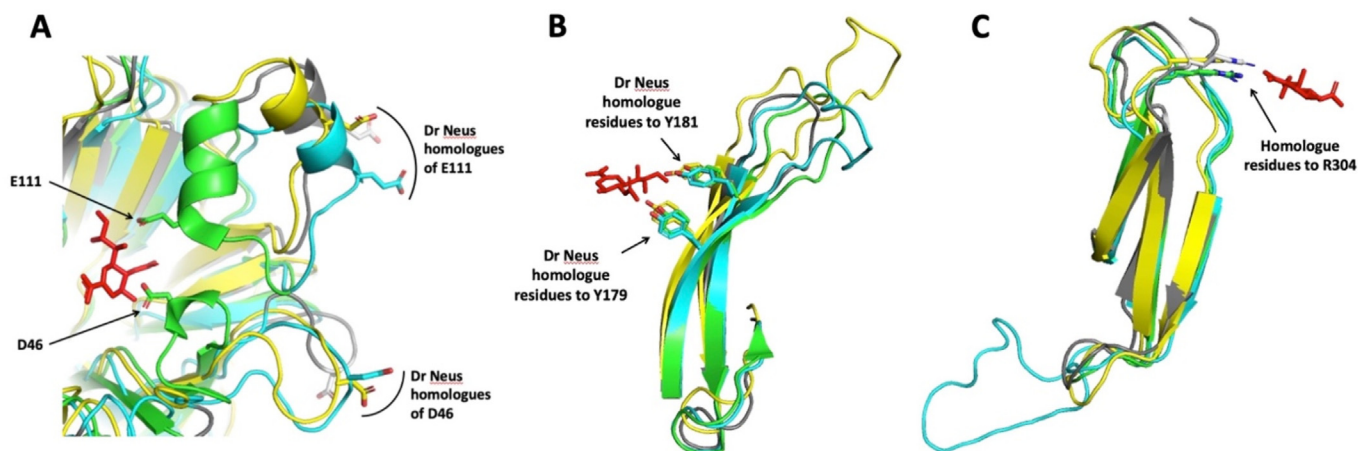

Fig. 7. Superimposition of portions of NEU2/DANA complex crystal structure (PDB ID 1VCU) with Dr Neus predicted structures.
(A) Overlapping of Hs NEU2 portion bearing the D46 and E111 residues with Dr Neu3.1, 2 and 3. The competitive inhibitor DANA interacts with the side chains of these acidic residues, located in α-helix portions of two mobile loops [13]. The homologue residues of Dr Neus 3D models are located in loops far away from the active site crevice. An α-helix portion is present only in the loop containing E111, as expected by the sugar-induced form of Hs NEU2 (PBD ID 1SO7) used as a template for modelling.
(B) DANA interacts with the hydroxyl groups of tyrosine 179 and 181 and the aromatic residues, located in beta sheets B (174—182) and C (191—199) of the third blade of the propeller [13]. The homologue residue positions are highly conserved in Dr Neus. Note the variable and increasing length of the loop connecting the two antiparallel beta sheets. (C) DANA interacts with the side chain terminal portion of the arginine 304 [13] and the homologue residues of Dr Neus are located in topologically equivalent positions. Note the difference in the length of the loop connecting beta sheets A (275—280) and B (291—298) of the fifth blade of the propeller in Dr Neu3.1 compared to the other sialidases.
The amino acid numbers are referred to Hs NEU2 [13]. Color code: DANA red, Hs NEU2 green; Dr Neu3.1 light blue; Dr Neu3.2 grey and Dr Neu3.3 yellow.

(Fig. 2). This behavior seems to be peculiar of these two zebrafish sialidases, since there are no evidences of aggregation in Hs NEU2 (data not shown). Again, the capacity of self-recognition of these paralogous proteins is probably due to the presence of loops of various length and peculiar amino acid composition connecting the antiparallel β-strands of the propeller (Fig. 5).

Substrate specificities of Dr Neu3.2 and Dr Neu3.3 shows interesting results. Despite the high degree of conservation of the pivotal residues in the active site architecture observed in the 3D models, these enzymes have different substrate preferences. Their activities toward three typical mammalian NEU3 ganglioside substrates, namely GD1a, GD3 and GM3, are different.

First of all, GD3 is the best substrate, followed by GD1a and GM3: apart GM3, the less acknowledged substrate from the paralogs and showing superimposable enzymatic activities, the remaining gangliosides show always higher activity when offered to Neu3.2 compared to Neu3.3. The activity on GD3 demonstrates that the two sialidase from zebrafish hydrolaze the α(2—8) glycosidic bond that links the external sialic acid residue to the inner in this particular glycosphingolipid. Surprisingly, the best substrate is GM1, recognized with an impressive difference by the two paralogs, a ganglioside that so far has been hydrolyzed only by HsNEU2 in monomeric dispersion [17], whereas in the experimental conditions used, the monosialylated GM1 is offered to zebrafish enzymes

as mixed micelle with Triton X-100 as the other gangliosides. Neu3.3 shows a specific activity toward GM1, corresponding to the 5% of the one detected using Neu3.2 and superimposable with the value observed for GD1a. The activity on fetuin and mucin support the hypothesis that the release of sialic acid from glycoproteins is influenced by the configuration of the glycosidic bonds, namely α(2−3) and α(2−6), and by the overall structure of the oligosaccharide antenna, namely N-glycans and O-glycans. Finally, although with the usual differences between the two zebrafish paralogs, an impressive activity toward α(2−3) sialyllactose is detectable. A comparison between these results and the previously characterized human NEU3 is not easy due the different experimental conditions used [27]. Nevertheless, the human counterpart is not able to remove sialic acid from GM1 and among gangliosides GM3 is the preferred substrate, followed by GD1a. Similar results have been obtained in vivo, upon transient transfection of NEU3 of mouse origin in COS7 cells [28]. In these conditions, the ganglioside cell contents clearly indicated that GD1a and GM3 are the best natural substrates of NEU3 and the enzyme is able to modify the ganglioside pattern also in neighboring cells. It is worth comparing our results on Neu3.2 and Neu3.3 from Danio rerio with those obtained in other species of teleosts used as animal models. By considering Neu3a and Neu3b from medaka (Oryzias latipes) subjected to stable expressed in HEK293 cells and Neuro2a cells [4], Neu3 enzymes show the highest activity on a ganglioside mixture, followed by colominic acid and 3-sialyllactose. Noteworthy, the activity on fetuin, mucin and 6-sialyllactose is detectable, but very low compared to the other substrates tested. Concerning gangliosides, GD3, followed by GM3 and GD1a are the best substrates and, although with lower efficiency, GM1 is also converted to the corresponding asialo-derivative by these enzymes. A similar picture is observed in the case of Neu3a from Nile tilapia (Oreochromis niloticus) transiently expressed in HEK293 cells, with GD3 ganglioside as the best substrate, followed by GD1a and GM3 and again a very low but well detectable activity toward GM1 [10]. Although the method used to measure the amount of sialic acid released by the enzyme activity is different from that used in our study, the sialidase activities toward gangliosides are comparable. These results support the notion that interactions between substrates and the enzyme surface, probably the area surrounding the active site crevice, are very important in determining the catalytic efficiency, as well as the aggregation state of gangliosides, as previously demonstrated using the purified human cytosolic sialidase NEU2 [17]. In particular, the kinetic parameters Vmax and Km measured with 4MU-NANA as substrate on Neu3.2 and Neu3.3 clearly show that Km has values comparable in all the enzymes, in the mM range of concentration, whereas the Vmax of the zebrafish enzymes are very low, less than 4%, compared to the one observed in HsNEU2. These wide discrepancies are typical of NEU3 proteins that showed much lower enzyme activities toward the artificial fluorescent substrate when compared to gangliosides [27]. Actually, the plasma membrane associated sialidase NEU3 of mammalian origin has been also named ganglioside sialidase for its typical high specificity toward ganglioside [29,30].

Focusing on the enzyme expression patterns the role(s) played by Neu3 in bony fishes can be better understood. In zebrafish RT-PCR experiments demonstrated that neu3.1 transcripts were detectable from 2 to 24 hpf during embryo development as well as in adult fish, whereas neu3.2 and neu3.3 transcripts were detectable at 24 hpf and from 12 hpf, respectively [3]. In addition, in situ hybridization experiments demonstrated that neu3.1 transcript is specifically localized in the gut from 24 hpf until 6 dpf [3]. More precise expression data on zebrafish sialidase can be extracted from the "Baseline expression from transcriptional profiling of zebrafish developmental stages" RNA-Seq dataset, generated by the Wellcome Trust Sanger Institute [22]. RNA-Seq data revealed that neu3.1 and neu3.2 are maternal genes, being expressed in the zygote and at 2- and at 128-cell stages (Fig. 8). When the zygotic gene transcription is activated, neu3.1 and neu3.2 transcript concentration initially drops to steadily increase again during development, with neu3.2 showing a higher level of transcription compared to neu3.1. Conversely, neu3.3 transcripts start to appear only at the late stages of development (72 hpf). Fig. 8 also reports the level of expression of neu1, encoding the lysosomal enzyme isoform, as a sialidase reference gene.

Concerning medaka, in adult animals neu3a and neu3b transcripts are detectable by RT-PCR in brain, liver and muscle with the first two tissues more active toward a ganglioside mixture than muscle [4]. Using the same technique, in adult Nile tilapia neu3a, neu3d and neu3e genes are differentially expressed in brain, heart, eye, liver, muscle and spleen [10].

More recently, a paper has provided a glycosylation map of adult zebrafish together with the expression pattern of enzymes involved in the metabolism of sialoglycoconjugates, giving to scientific community an impressive amount of data to better understand glycans function in this animal model [31]. In particular, the eight tissues studied revealed specific glycosylation patterns linked to a defined expression pattern of the genes encoding the enzymes involved in sialic acid metabolism. Noteworthy, neu3 genes are expressed in most or all the tissues studied, with relative transcript levels ranging from intermediate to strong. From these evidences, also Neu3.4 and Neu3.5 are sialidases that will deserve an accurate biochemical characterization.

Concerning the possible role played by Neu3s in bony fishes, in medaka Neu3a played a relevant role in neurite formation in Neuro2a cells upon administration of retinoic acid, whereas Neu3b had not effect and behaved as a soluble enzyme [4], similarly to zebrafish Neu3.2 [3], supporting the hypothesis that it represents a phylogenetic precursor of the cytosolic sialidase NEU2 [2].

Moreover, Neu3b is highly conserved in medaka and tilapia and its overexpression in mouse myoblast C2C12 cells enhanced differentiation to myotubes [7]. Myoblasts expressing Neu3b showed a decrease in GM2 and an increase of Lac-Cer, resulting in a decline in EGFR/ERK phosphorylation. These results support the involvement of Neu3b as a positive regulator for myoblast differentiation, similar to mammalian cytosolic sialidase NEU2. The role played by NEU2 in skeletal muscle cell differentiation has been demonstrated for the first time in rat L6 myoblast differentiation [32], followed by a study on murine C2C12 myoblasts [33]. In addition, the enzyme activity and its transcript levels in hypertrophic myofibers or in myofiber atrophy, increase and decrease respectively [34], demonstrating that Neu2 levels are pivotal for in vitro correct muscle differentiation and growth. Based on these evidences, it is intriguing to better characterize Neu3.2 as the soluble member of zebrafish neu3 gene cluster and thus a possible functional ortholog of NEU2 in higher vertebrates [2]. As already reported, zebrafish neu3.2 is part of a cluster of a five tandemly repeated NEU3-like genes likely originated by unequal recombination [3]. Only two NEU3-like genes are described in medaka: neu3a on Chr 14, in a region syntenic to the neu3.1-5 zebrafish cluster on Chr 21, while neu3b is on Chr 12. A phylogenetic analysis carried out by Shiozaki ed al. indicates that medaka neu3a was relatively close to zebrafish neu3.1, while medaka neu3b was not, suggesting that the medaka neu3b was independently evolved in this teleost [4].

In general, these results provide another piece of information about sialidases and their role in the intriguing pictures of sialic acid biology in bony fish. Further studies are ongoing in our laboratory to better understand their possible role during zebrafish embryo development with particular regard to Dr Neu3.2 in muscle differentiation.
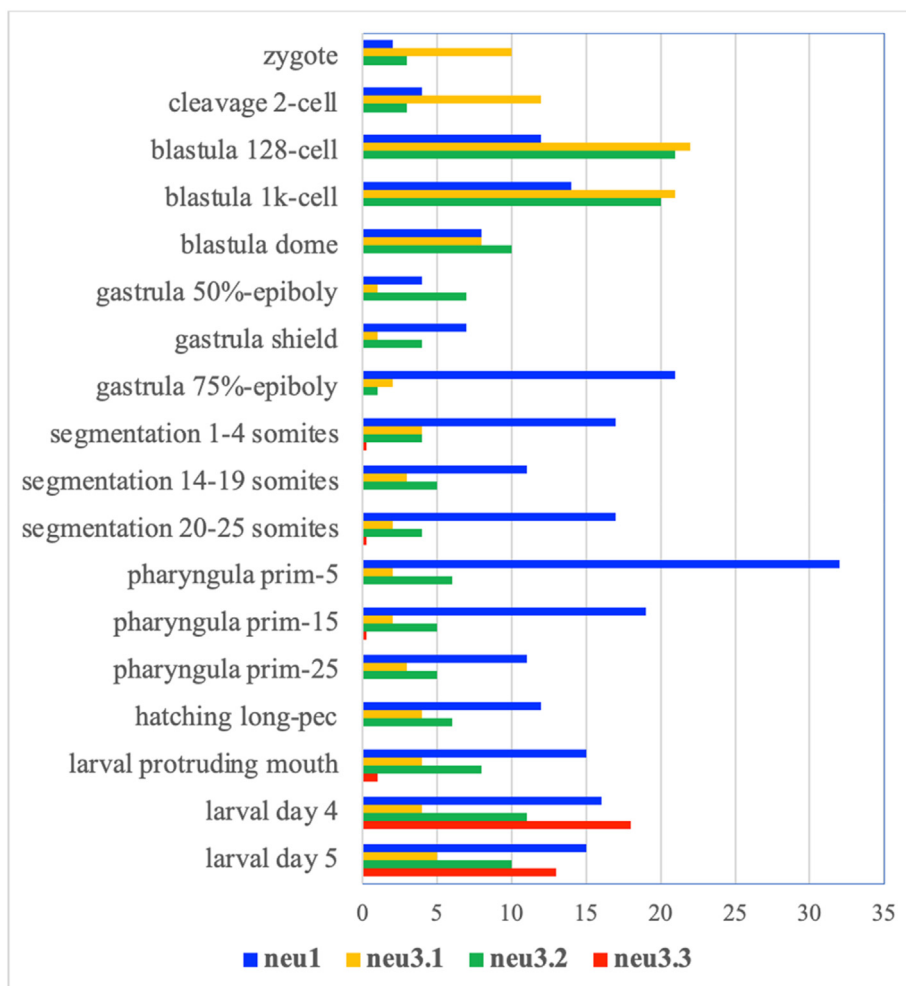
Fig. 8. Expression levels of neu1, neu3.1, neu3.2 and neu3.3 sialidase genes during zebrafish development.
The temporal expression profiles were extracted from the "Baseline expression from transcriptional profiling of zebrafish developmental stages" RNA-Seq dataset generated by the Wellcome Trust Sanger Institute [27]. The study produced temporal expression profiles of 23,642 zebrafish genes across 18 developmental time points (from 1 cell to 5 days post-fertilization) sampling individual and pools of embryos (5 biological replicate per time point). On the X-axis, normalized transcript counts per gene are expressed as Transcripts Per Million (TPM).

5. Conclusions

Sialidases have been studied in several bony fishes and these organisms represent an important tool to study the roles played by these enzymes in different biological environments. Our biochemical characterization of Dr Neu3.2 and Neu3.3 demonstrated a peculiar aggregation behavior of these enzymes, as well as different substrate specificities apart from GM3 a 3-sialyllactose. These different features of the two sialidases from zebrafish are due to the primary structure of each protein and the corresponding 3D structure of the enzymes. A study of Dr Neu3.1, Neu3.2 and Neu3.3 3D structure models, obtained using the crystal structure of Hs NEU2 as a template, demonstrated that the differences among these enzymes are located in the loops connecting the antiparallel beta-stands of the six bladed propeller core. These portions are probably involved in substrate specificity and aggregation behavior, determining either cytosolic or membrane associated subcellular localization when expressed in mammalian cells and soluble or inclusion bodies localization, when expressed as recombinant proteins in *E. coli*. An *in silico* analysis of the RNA-Seq expression data available on the genes encoding the three sialidases from zebrafish revealed other interesting pieces of information. In fact,

neu3.1, neu3.2 and *neu3.3* transcripts showed peculiar expression patterns during embryogenesis, strongly supporting the notion of different specific roles of these sialidases in the different stages of development.

These results offer interesting hints about the biology of sialidases and the role played by sialoglycoconjugates in a variety of events. Further experiments will be carried out to better understand the role played by these Neu3 enzymes in *Danio rerio*.

Author contributions

Conceptualization, M.F, M.M., P.F. R.B., G.B. and E.M.; investigation, M.F., M.M., G.B., M.B., N.P. and P.F.; molecular modelling, M.B. and E.G.; *in silico* analysis, G.B.; resources, R.B., P.F., G.B. and E.M.; writing original draft preparation, M.F. and E.M.; writing, reviewing

and editing, M.F., M.M., R.B., P.F., G.B. and E.M.; visualization, M.F., G.B. and E.M.; supervision, M.F. and E.M.

Note

The views expressed are those of the authors and not necessarily those of the NIHR or the Department of Health and Social Care.

Declaration of interests

Manuscript entitled "Characterization of three sialidases from *Danio rerio*".

By Matilde Forcella, Marta Manzoni, Giuliana Benaglia, Marcella Bonanomi, Edoardo Giacopuzzi, Nadia Papini, Roberto Bresciani, Paola Fusi, Giuseppe Borsani and Eugenio Monti.

The authors declare that they have no known competing financial interests or personal relationships that could have appeared to influence the work reported in this paper.

Appendix A. Supplementary data

Supplementary data to this article can be found online at https://doi.org/10.1016/j.biochi.2021.05.005.

References

[1] E. Monti, E. Bonten, A. D'Azzo, R. Bresciani, B. Venerando, G. Borsani, R. Schauer, G. Tettamanti, Sialidases in vertebrates: a family of enzymes tailored for several cell functions, Adv. Carbohydr. Chem. Biochem. 64 (2010) 403—479.

[2] E. Giacopuzzi, R. Bresciani, R. Schauer, E. Monti, G. Borsani, New insights on the sialidase protein family revealed by a phylogenetic analysis in metazoa, PloS One 7 (2012), e44193.

[3] M. Manzoni, P. Colombi, N. Papini, L. Rubaga, N. Tiso, A. Preti, B. Venerando, G. Tettamanti, R. Bresciani, F. Argenton, G. Borsani, E. Monti, Molecular cloning and biochemical characterization of sialidases from zebrafish (Danio rerio), Biochem. J. 408 (2007) 395—406.

[4] K. Shiozaki, K. Takeshita, M. Ikeda, A. Ikeda, Y. Harasaki, M. Komatsu, S. Yamada, K. Yamaguchi, T. Miyagi, Molecular cloning and biochemical characterization of two novel Neu3 sialidases, neu3a and neu3b, from medaka (Oryzias latipes), Biochimie 95 (2013) 280—289.

[5] K. Shiozaki, S. Ryuzono, N. Matsushita, A. Ikeda, K. Takeshita, P.K. Chigwechokha, M. Komatsu, T. Miyagi, Molecular cloning and biochemical characterization of medaka (Oryzias latipes) lysosomal neu4 sialidase, Fish Physiol. Biochem. 40 (2014) 1461—1472.

[6] S. Ryuzono, R. Takase, K. Oishi, A. Ikeda, P.K. Chigwechokha, A. Funahashi, M. Komatsu, T. Miyagi, K. Shiozaki, Lysosomal localization of Japanese medaka (Oryzias latipes) Neu1 sialidase and its highly conserved enzymatic profiles with human, Gene 575 (2016) 513—523.

[7] K. Shiozaki, Y. Harasaki, M. Fukuda, A. Yoshinaga, S. Ryuzono, P.K. Chigwechokha, M. Komatsu, T. Miyagi, Positive regulation of myoblast differentiation by medaka Neu3b sialidase through gangliosides desialylation, Biochimie 123 (2016) 65—72.

[8] S. Ryuzono, R. Takase, Y. Kamada, T. Ikenaga, P.K. Chigwechokha, M. Komatsu, K. Shiozaki, Suppression of Neu1 sialidase delays the absorption of yolk sac in medaka (Oryzias latipes) accompanied with the accumulation of alpha2-3 sialo-glycoproteins, Biochimie 135 (2017) 63—71.

[9] K. Oishi, M. Miyazaki, R. Takase, P.K. Chigwechokha, M. Komatsu, K. Shiozaki, Regulation of triglyceride metabolism in medaka (Oryzias latipes) hepatocytes by Neu3a sialidase, Fish Physiol. Biochem. 46 (2020) 563—574.

[10] P.K. Chigwechokha, M. Komatsu, T. Itakura, K. Shiozaki, Nile Tilapia Neu3 sialidases: molecular cloning, functional characterization and expression in Oreochromis niloticus, Gene 552 (2014) 155—164.

[11] A. Honda, P.K. Chigwechokha, Y. Kamada-Futagami, M. Komatsu, K. Shiozaki, Unique nuclear localization of Nile tilapia (Oreochromis niloticus) Neu4 sialidase is regulated by nuclear transport receptor importin alpha/beta, Biochimie 149 (2018) 92—104.

[12] A. Honda, P.K. Chigwechokha, R. Takase, O. Hayasaka, K. Fujimura, T. Kotani, M. Komatsu, K. Shiozaki, Novel nile tilapia Neu1 sialidases: molecular cloning

[13] L.M. Chavas, C. Tringali, P. Fusi, B. Venerando, G. Tettamanti, R. Kato, E. Monti, S. Wakatsuki, Crystal structure of the human cytosolic sialidase Neu2. Evidence for the dynamic nature of substrate recognition, J. Biol. Chem. 280 (2005) 469—475.

[14] M.R. Green, J. Sambrook, Molecular Cloning: A Laboratory Manual, fourth ed., Cold Spring Harbor Laboratory Press, Cold Spring Harbor, NY, 2012.

[15] E. Monti, A. Preti, C. Nesti, A. Ballabio, G. Borsani, Expression of a novel human sialidase encoded by the NEU2 gene, Glycobiology 9 (1999) 1313—1321.

[16] U.K. Laemmli, Cleavage of structural proteins during the assembly of the head of bacteriophage T4, Nature 227 (1970) 680—685.

[17] C. Tringali, N. Papini, P. Fusi, G. Croci, G. Borsani, A. Preti, P. Tortora, G. Tettamanti, B. Venerando, E. Monti, Properties of recombinant human cytosolic sialidase HsNEU2. The enzyme hydrolyzes monomerically dispersed GM1 ganglioside molecules, J. Biol. Chem. 279 (2004) 3169—3179.

[18] L. Warren, The thiobarbituric acid assay of sialic acid, J. Biol. Chem. 234 (1959) 1971—1975.

[19] B. Venerando, A. Fiorilli, G.L. Croci, G. Tettamanti, Presence in human erythrocyte membranes of a novel form of sialidase acting optimally at neutral pH, Blood 90 (1997) 2047—2056.

[20] S.K. Burley, H.M. Berman, C. Bhikadiya, C. Bi, L. Chen, L. Di Costanzo, C. Christie, K. Dalenberg, J.M. Duarte, S. Dutta, Z. Feng, S. Ghosh, D.S. Goodsell, R.K. Green, V. Guranovic, D. Guzenko, B.P. Hudson, T. Kalro, Y. Liang, R. Lowe, H. Namkoong, E. Peisach, I. Periskova, A. Prlic, C. Randle, A. Rose, P. Rose, R. Sala, M. Sekharan, C. Shao, L. Tan, Y.P. Tao, Y. Valasatava, M. Voigt, J. Westbrook, J. Woo, H. Yang, J. Young, M. Zhuravleva, C. Zardecki, RCSB Protein Data Bank: biological macromolecular structures enabling research and education in fundamental biology, biomedicine, biotechnology and energy, Nucleic Acids Res. 47 (2019) D464—D474.

[21] L. Zimmermann, A. Stephens, S.Z. Nam, D. Rau, J. Kubler, M. Lozajic, F. Gabler, J. Soding, A.N. Lupas, V. Alva, A completely reimplemented MPI bioinformatics toolkit with a new HHpred server at its core, J. Mol. Biol. 430 (2018) 2237—2243.

[22] R.J. White, J.E. Collins, I.M. Sealy, N. Wali, C.M. Dooley, Z. Digby, D.L. Stemple, D.N. Murphy, K. Billis, T. Hourlier, A. Fullgrabe, M.P. Davis, A.J. Enright, E.M. Busch-Nentwich, A high-resolution mRNA expression time course of embryonic development in zebrafish, Elife (2017) 6.

[23] A. Buschiazzo, P.M. Alzari, Structural insights into sialic acid enzymology, Curr. Opin. Chem. Biol. 12 (2008) 565—572.

[24] L.M. Chavas, R. Kato, N. Suzuki, M. von Itzstein, M.C. Mann, R.J. Thomson, J.C. Dyason, J. McKimm-Breschkin, P. Fusi, C. Tringali, B. Venerando, G. Tettamanti, E. Monti, S. Wakatsuki, Complexity in influenza virus targeted drug design: interaction with human sialidases, J. Med. Chem. 53 (2010) 2998—3002.

[25] A. Sali, T.L. Blundell, Comparative protein modelling by satisfaction of spatial restraints, J. Mol. Biol. 234 (1993) 779—815.

[26] A.K. Upadhyay, A. Murmu, A. Singh, A.K. Panda, Kinetics of inclusion body formation and its correlation with the characteristics of protein aggregates in Escherichia coli, PloS One 7 (2012), e33951.

[27] E. Monti, M.T. Bassi, N. Papini, M. Riboni, M. Manzoni, B. Venerando, G. Croci, A. Preti, A. Ballabio, G. Tettamanti, G. Borsani, Identification and expression of NEU3, a novel human sialidase associated to the plasma membrane, Biochem. J. 349 (2000) 343—351.

[28] N. Papini, L. Anastasia, C. Tringali, G. Croci, R. Bresciani, K. Yamaguchi, T. Miyagi, A. Preti, A. Prinetti, S. Prioni, S. Sonnino, G. Tettamanti, B. Venerando, E. Monti, The plasma membrane-associated sialidase MmNEU3 modifies the ganglioside pattern of adjacent cells supporting its involvement in cell-to-cell interactions, J. Biol. Chem. 279 (2004) 16989—16995.

[29] T. Hasegawa, K. Yamaguchi, T. Wada, A. Takeda, Y. Itoyama, T. Miyagi, Molecular cloning of mouse ganglioside sialidase and its increased expression in Neuro2a cell differentiation, J. Biol. Chem. 275 (2000) 8007—8015.

[30] T. Miyagi, K. Takahashi, K. Yamamoto, K. Shiozaki, K. Yamaguchi, Biological and pathological roles of ganglioside sialidases, Prog Mol Biol Transl Sci 156 (2018) 121—150.

[31] N. Yamakawa, J. Vanbeselaere, L.Y. Chang, S.Y. Yu, L. Ducrocq, A. Harduin-Lepers, J. Kurata, K.F. Aoki-Kinoshita, C. Sato, K.H. Khoo, K. Kitajima, Y. Guerardel, Systems glycomics of adult zebrafish identifies organ-specific sialylation and glycosylation patterns, Nat. Commun. 9 (2018) 4647.

[32] K. Sato, T. Miyagi, Involvement of an endogenous sialidase in skeletal muscle cell differentiation, Biochem. Biophys. Res. Commun. 221 (1996) 826—830.

[33] A. Fanzani, R. Giuliani, F. Colombo, D. Zizioli, M. Presta, A. Preti, S. Marchesini, Overexpression of cytosolic sialidase Neu2 induces myoblast differentiation in C2C12 cells, FEBS Lett. 547 (2003) 183—188.

[34] A. Fanzani, R. Giuliani, F. Colombo, S. Rossi, E. Stoppani, W. Martinet, A. Preti, S. Marchesini, The enzymatic activity of sialidase Neu2 is inversely regulated during in vitro myoblast hypertrophy and atrophy, Biochem. Biophys. Res. Commun. 370 (2008) 376—381.